

## §58. The Profiles of the Divertor Heat Load for Various Operations in LHD

Masuzaki, S., Sakamoto, R., Morisaki, T., Kubota, Y., Noda, N.

The built-in divertor in the heliotron-type magnetic configuration has 3-dimensional structure, and the particle and power deposition profiles on it are not uniform even in the helical direction.

Heat deposition profiles on the helical divertor are investigated using thermocouples embedded in divertor plates at different positions in the helical direction as shown in Fig.1(a). Temperature rises of the divertor plates ( $\Delta T$ ) which contact two divertor legs (see Fig.1(b)) were measured for various operations.

Figure 2(a) and (b) show the normalized temperature rises ( $\Delta T$ ) at those divertor plates in the NBI heated discharges of  $R_{ax} = 3.6$  m and 3.75 m with  $B_t = 2.75$  T and 2.64 T, respectively, as functions of toroidal angle. The difference of the heat deposition profiles for  $R_{ax}$  is clearly shown. For the case of  $R_{ax} = 3.75$  m, the dominant positions of the heat deposition are top and bottom divertor. On the other hand, it is inboard-side divertor for the case of  $R_{ax} = 3.6$  m. These trends are same as the particle deposition profiles. The numerical results of field line tracing with random walk process were carried out [1,2] to simulate the particle deposition on the helical divertor. The trends of the particle deposition profiles measured by Langmuir probes agree with this calculated results qualitatively [3]. In Figs.2, the results of that calculation are also shown. The normalized  $\Delta T$  profiles also agree with the numerical results qualitatively.

In Heliotron-E, large up-down asymmetry of the diverted plasma was observed [4,5]. The particle flux to bottom-side collector plates were larger than that to up-side collector plates up to factor of 10. However in LHD, such large asymmetry has not been observed at least in  $\Delta T$  profile in present operation regime.

Figure 2(c) shows  $\Delta T$  profiles for the discharges with  $R_{ax} = 3.6$  m and  $B_t = 0.5$  T. In spite of the same magnetic configuration, the heat deposition profiles of Fig.2(a) and (c) are clearly different each other. This difference is considered to be caused by the relatively high  $\beta$  in the low field discharge. In Fig.2(c), the range of  $\langle\beta\rangle$  is 2.5% to 3.2%. On the other hand, it is below 0.9% in Fig.2(a). For the high  $\beta$  discharge, the dominant positions of heat deposition are top and bottom divertor, and this heat deposition profile is similar to that for the discharge of  $R_{ax} = 3.75$  m which is shown in Fig.2(b). The trend of the modification of the heat deposition profile is qualitatively agree with that of the particle deposition profile measured by Langmuir probe arrays. Shafranov-shift for high  $\beta$  is seems to cause this modification of heat deposition profile.

### References

- [1] Ohyabu, N., et al., Nucl. Fusion 34 (1994) 387.
- [2] Morisaki, T., et al., in Proc. 27th EPS (2000) 1345.
- [3] Masuzaki, S., et al., J. Nucl. Mater. 290-293 (2001) 12.
- [4] Mizuuchi, T., et al., J. Nucl. Mater. 266-269 (1999) 1139.
- [5] Chechkin, V., et al., Nucl. Fusion 40 (2000) 796.

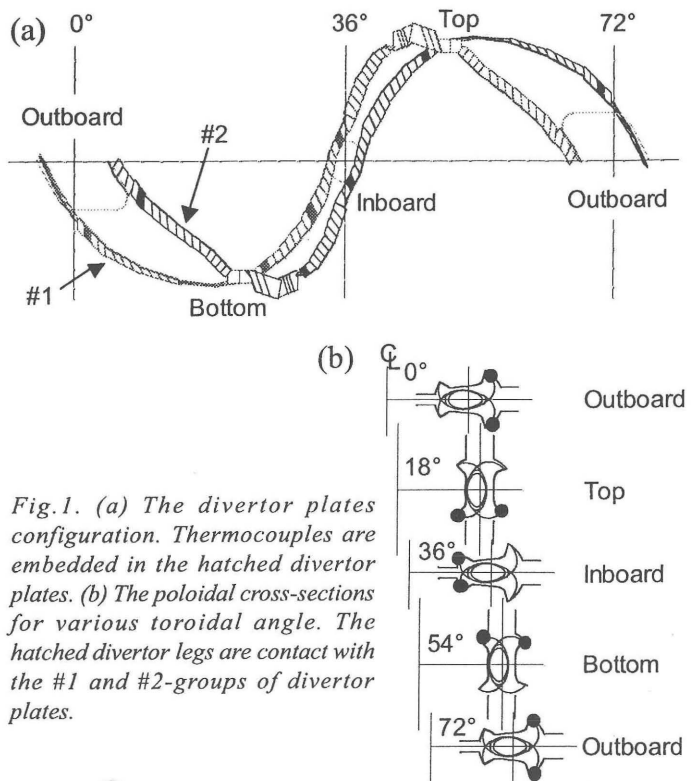


Fig.1. (a) The divertor plates configuration. Thermocouples are embedded in the hatched divertor plates. (b) The poloidal cross-sections for various toroidal angle. The hatched divertor legs are contact with the #1 and #2-groups of divertor plates.

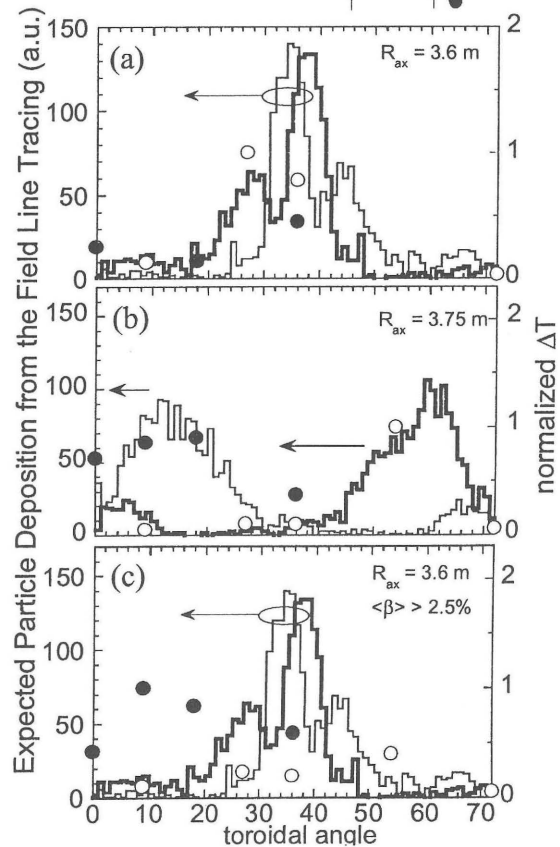


Fig.2: Normalized temperature rise of the divertor plates (symbols) at various positions and the expected particle deposition profiles from the results of the field line tracing under the vacuum condition (lines) against toroidal angle. Thin lines and closed circles are for #1-group of divertor plates, and bold lines and open circles are for #2-group. (a)  $R_{ax}=3.6$  m. (b)  $R_{ax}=3.75$  m. (c)  $R_{ax}=3.6$  m and  $2.5\% < \langle\beta\rangle < 3.2\%$ .